Supplementary Information

Lesion Distribution

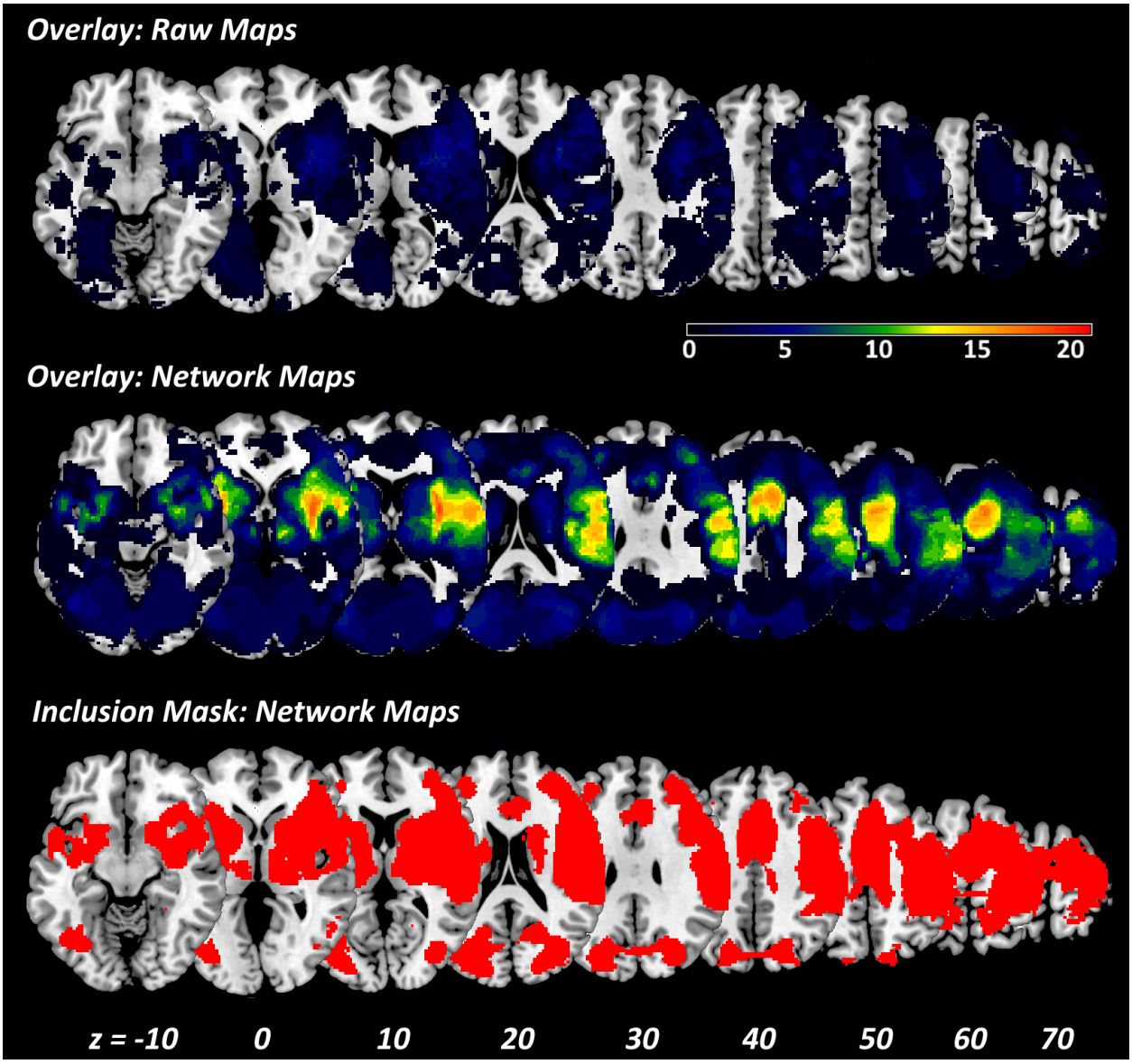

Supplementary Figure 1. Axial sections of standard MNI brain describing: the overlap of all lesion masks from the patients tested (first line); the overlap of all network masks from the patient tested (second line); the regions involved in the analysis (third line), as described with those implicated in the network maps of with at least 10% of patients (N = 4).

Independent Component Analysis of functional data

We run group-independent component analysis (ICA) as implemented in the toolbox GIFT 4.0a (https://trendscenter.org/software/gift/). More specifically, subjects' data were reduced to a lower dimensionality by using a two-stage principal component analysis (one at an individual level and one at a group level). Then, data from all subjects/sessions were concatenated and 20 independent group components were estimated using the Infomax approach (Bell & Sejnowski, 1995). Supplementary Figure 2 shows an example of 2 high-frequency artefactual components (n. 7 and 15), characterized by a "striped" spatial distribution possibly related to MRI acquisition/reconstruction. These two artefactual components were removed by the preprocessed data prior the NLSM.

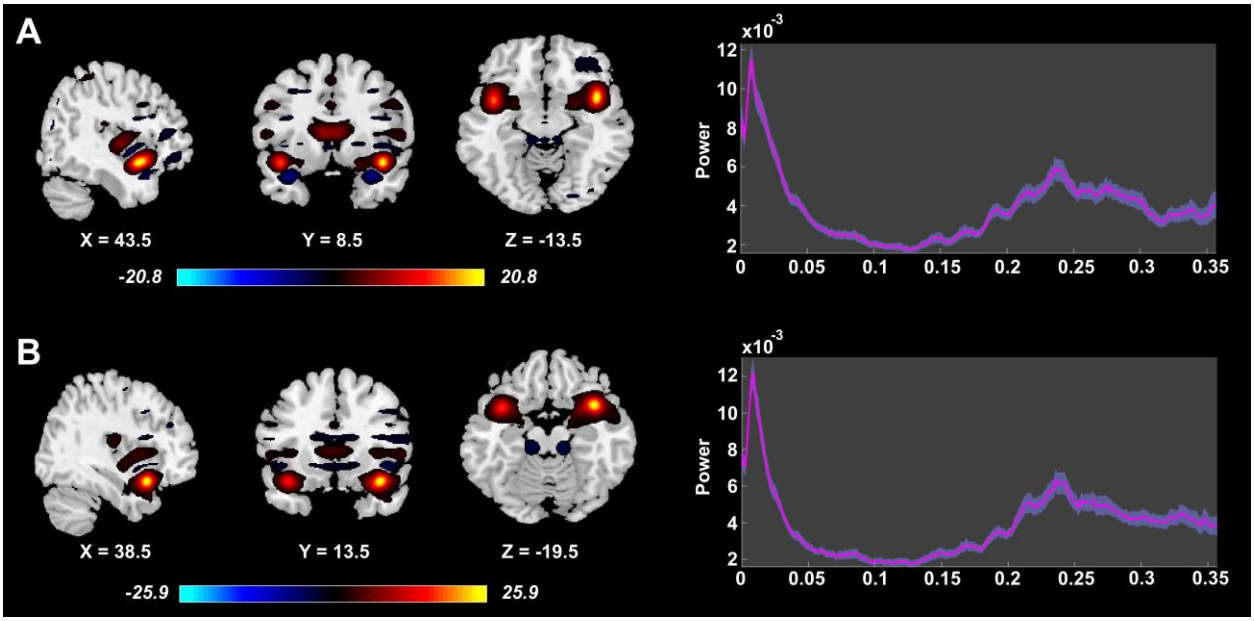

Supplementary Figure 2. Two artefactual independent components which were removed from the Resting State dataset prior the analysis. Each component is described through orthogonal slices, as well as through average (plus standard deviation area) power spectra across all subjects/sessions.

Supplementary Behavioral Analysis

We extended the analysis described in section 3.1 by running a Repeated Measures ANOVA with Condition (*Ph*, *B*, *E*, and *Pa*) as within-subject factor, Group (Left-damaged Patients, Right-damaged Patients and Controls) as between-subjects factor, and age or educational level as covariate. The inclusion of either of these variables as covariate had no influence on the effects described in section 3.1, with Condition and Groups still being found to be significant ($F \geq 4.26$, $p \leq 0.019$, $\eta_p^2 \geq 0.09$), and Group*Condition not ($F \leq 0.51$, $p \geq 0.801$, $\eta_p^2 \leq 0.02$). As for the covariate themselves, education and age had no impact on the accuracy, neither as a main effects nor in interaction with Group/Condition ($F \leq 2.94$, $p \geq 0.092$, $\eta_p^2 \leq 0.05$).

We focused on the patients' data and repeated the ANOVA including patients' global cognitive efficiency score (from MoCA) or the time post-strike, as covariates. These analyses revealed only a MoCA*Condition interaction ($F_{(3,96)} = 2.76$, $p = 0.047$, $\eta_p^2 = 0.08$), whereas no other effect was found to be significant ($F \leq 3.89$, $p \geq 0.057$, $\eta_p^2 \leq 0.10$; except for the Condition main effect observed already in the previous ANOVAs, $F \geq 3.42$, $p \leq 0.021$, $\eta_p^2 \leq 0.10$). This interaction was further explored by calculating a correlation coefficient between MoCA score and participants' accuracy in each of the four conditions. Although none of these survived Bonferroni-correction for the four comparisons, it is interesting to note that only participants' performance in *B* correlated positively with the MoCA score (Pearson $r = 0.35$, $p = 0.038$; see Supplementary Figure 3B), whereas the other three conditions did not (*Ph, E, Pa*: $r \leq 0.21$, $p \geq 0.229$).

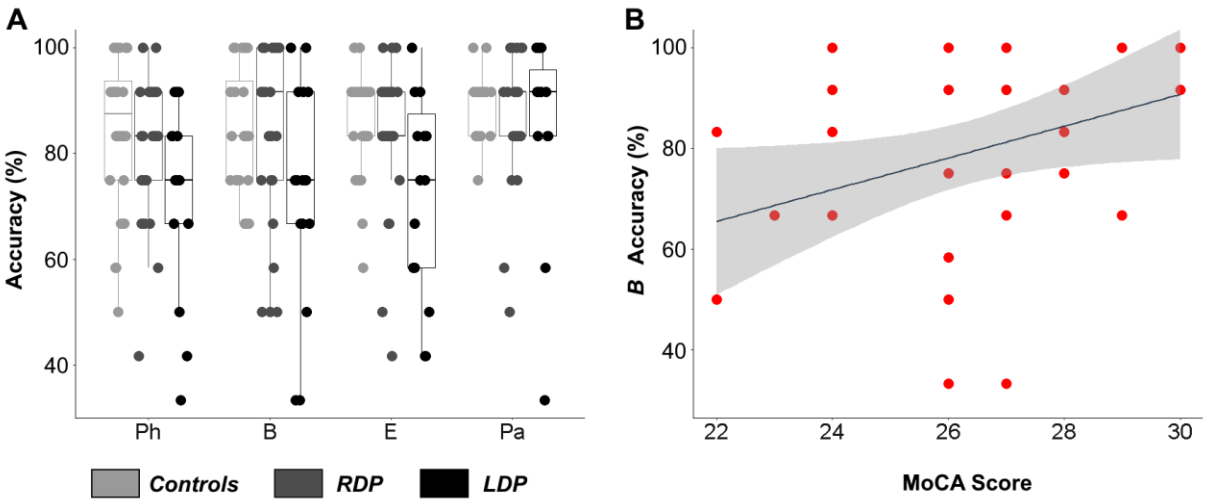

Supplementary Figure 3. (**A**) Boxplots plots showing the performance of controls (light gray), patients with damage to the right hemisphere (*RDP*, dark gray) and patients with damage to the left hemisphere (*LDP*, black). Boxplots are characterized by a horizontal line referring to the median of the distribution, a rectangle referring to the inter-quartile range, and whiskers referring to the overall data range (within 1.5 of the inter-quartile range). Individual data are also displayed as filled circles. (**B**) Scatter plot displaying patients' performance in the belief (*B*) condition, against MoCA Score. The relationship is displayed through linear regression with 95% confidence intervals area.

Effects Reliability and Power Analysis

Supplementary-Table 1. Reliability of the effects observed

	R^2	R^2-resamples	p value	p-resamples	Power	
					0.05	0.001
Effects of Beliefs *(covaring per Ph)*						
DLPFC	0.28	0.29 [0.20, 0.37]	$1.99 \cdot 10^{-4}$	1.93 [0.17,21.22]$\cdot 10^{-4}$	0.92	0.68
DMPFC	0.31	0.31 [0.22, 0.39]	$9.66 \cdot 10^{-5}$	9.54 [0.47, 109.4]$\cdot 10^{-5}$	0.92	0.74
Effects of Beliefs *(covaring per E)*						
DLPFC	0.33	0.33 [0.20, 0.43]	$4.60 \cdot 10^{-5}$	4.47 [0.19, 187.2]$\cdot 10^{-5}$	0.92	0.70
DMPFC	0.36	0.36 [0.23, 0.46]	$1.86 \cdot 10^{-5}$	2.11 [0.07, 92.22]$\cdot 10^{-5}$	0.94	0.75
Effects of Emotions *(covaring per Ph)*						
Anterior Insula	0.40	0.40 [0.28, 0.51]	$5.02 \cdot 10^{-6}$	6.25 [0.13, 206.5]$\cdot 10^{-6}$	0.98	0.84

For each region displayed in Table 3, we report the effect size (R^2) and the associated *p*-value (see Lorca-Puls et al., 2018). For each of these we also report median and inter-quartile range of the same measure obtained through 5000 bootstrap-resamples of the original dataset. Power is defined by the relative amount of times the *p*-value from the resampled dataset was smaller than 0.05 or 0.001

Supplementary-Table 2. Effect size as function of significance

	All Resamples	Resamples significant at:	
		0.05	0.001
Effects of Beliefs *(covaring per Ph)*			
DLPFC	0.29 [0.20, 0.37]	0.30 [0.22, 0.38]	0.35 [0.29, 0.41]
DMPFC	0.31 [0.22, 0.39]	0.32 [0.24, 0.40]	0.36 [0.29, 0.42]
Effects of Beliefs *(covaring per E)*			
DLPFC	0.33 [0.20, 0.43]	0.34 [0.23, 0.44]	0.39 [0.31, 0.44]
DMPFC	0.36 [0.23, 0.46]	0.37 [0.26, 0.47]	0.41 [0.33, 0.49]
Effects of Emotions *(covaring per Ph)*			
Anterior Insula	0.40 [0.28, 0.51]	0.40 [0.28, 0.51]	0.44 [0.33, 0.52]

For each simulation displayed in Supplementary Table 1, we report the median effect size (R^2) and interquartile range of all resamples, together with a subportion of those resamples significant at 0.05 or 0.001